ACS APPLIED MATERIALS & INTERFACES

Research Article

www.acsami.org

# pH- and Reduction-Responsive Polymeric Lipid Vesicles for Enhanced Tumor Cellular Internalization and Triggered Drug Release

Sheng Wang, Shuangnan Zhang, Junqing Liu, Zhongyun Liu, Lin Su, Hanjie Wang,* and Jin Chang*

Institute of Nanobiotechnology, School of Materials Science and Engineering, Tianjin University and Tianjin Key Laboratory of Composites and Functional Materials, Tianjin 300072, PR China

Supporting Information

**ABSTRACT:** Enhanced tumor cellular internalization and triggered drug release are two main concerns in the development of nanoparticles for antitumor drug delivery. In this article, a new kind of smart pH- and reduction-dual-responsive drug- loaded PEG coated polymeric lipid vesicle (PPLV) that can achieve both enhanced tumor cellular internalization and triggered drug release has been designed and prepared. The PPLVs were formed from amphiphilic dextran derivatives. The antitumor drug, doxorubicin (DOX), was loaded in the cores of the PPLVs. The newly developed PPLVs had a nanosized structure (~40 nm) with PEG coating, so they were neutral and had high colloidal stability in the blood circulation. The *in vitro* physicochemical characterizations showed that the PPLVs lose their PEG coating and expose the positive surface charge under acidic environments. The *in vitro* cellular uptake study indicated that the acidic-treated PPLVs can efficiently enter tumor cells. It has been demonstrated by *in vitro* DOX release profiles that the PPLVs can achieve a triggered drug release in response to the reduction environment. The MTT assay demonstrated that DOX-loaded PPLVs treated with pH 5.0 solution had higher antitumor activity than DOX-loaded PPLVs treated with pH 7.4 solution. These results suggested that the PPLVs were promising nanoparticles for smart antitumor drug delivery applications.

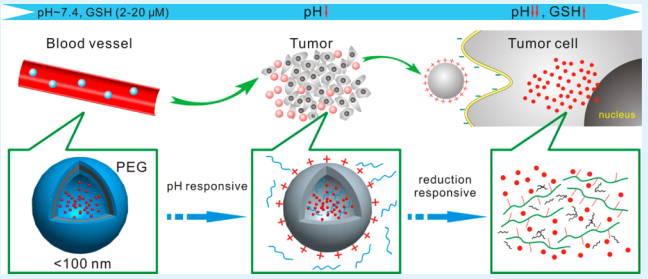


**KEYWORDS:** *polymeric lipid vesicle, dual-responsive, drug delivery, enhanced cellular internalization, triggered release*

## 1. INTRODUCTION

Nanoparticles, have emerged as one of the most fascinating drug delivery systems for the controlled delivery of antitumor drugs to improve therapeutic efficacy and reduce systemic toxicity.[1−3] The design and development of "intelligent" nanoparticles seek to expand upon the benefits.[4,5] There are two main concerns in the development of nanoparticles for antitumor drug delivery: enhanced tumor cellular internalization and triggered drug release.

To achieve enhanced tumor cellular internalization, the designed nanoparticles should effectively accumulate into tumor tissues and then rapidly enter the tumor cells. Many properties of nanoparticles play a significant role in determining biodistribution and particle−cell interactions, wherein the surface charge is an important factor.[6−8] Generally speaking, neutral or negatively charged nanoparticles exhibit higher colloidal stability and longer circulation time than positively charged nanoparticles.[9−11] So they easily accumulate into tumor tissues by the enhanced permeability and retention (EPR) effect. Nevertheless, neutral or negatively charged nanoparticles cannot effectively enter the cells. In contrast, numerous studies have shown that positively charged nanoparticles are more efficient at cellular internalization than neutral and negatively charged nanoparticles because of their effective binding to negatively charged cell membranes through electrostatic interactions.[8] For example, DeSimone et al. investigated the effect of nanoparticle surface charge on cellular internalization. The results indicated that positively charged nanoparticles were internalized in 84% of cells after a 1-h incubation period, whereas the negatively charged nanoparticles were not internalized to any significant amount (<5%).[12] Therefore, the design of a surface charge-switchable nanoparticle that shows neutral or negative surface charge in circulation and shows positive surface charge in the tumor site is an important way to realize enhanced tumor cellular internalization.

To achieve triggered drug release, various responsive nanoparticles that can respond to certain stimulation (e.g., pH, redox, and temperature) and then release the encapsulated drugs have been actively pursued.[13−15] These nanoparticles usually consist of biodegradable polymers that contain characteristic chemical bonds in the molecular chains. In circulation, these chemical bonds are stable, whereas they are prone to rapid break down in certain tumor stimulating environments. For example, in the cytosol and cell nuclei, the concentration of glutathione (GSH) is 2−10 mM, maintaining a high reduction environment inside cells; while in body fluids and in the extracellular milieu, the concentration of GSH is

Received: April 28, 2014
Accepted: June 18, 2014
Published: June 18, 2014

**Scheme 1. Schematic Illustration Showing the Whole Procedure for the PPLVs into the Tumor Cells**

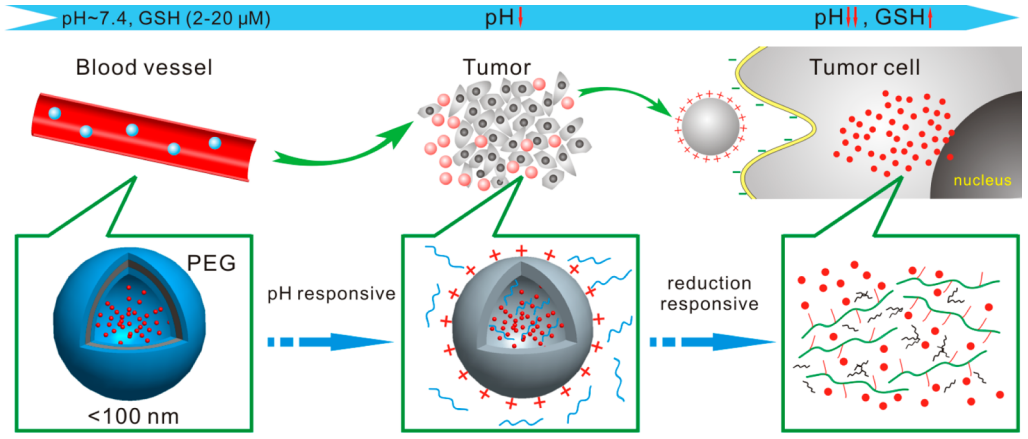


**Scheme 2. Synthesis Process of $C_{18}$-*S*-*S*-COOH (A), DS (B), LDS (C), and PEG-oDS (D)**

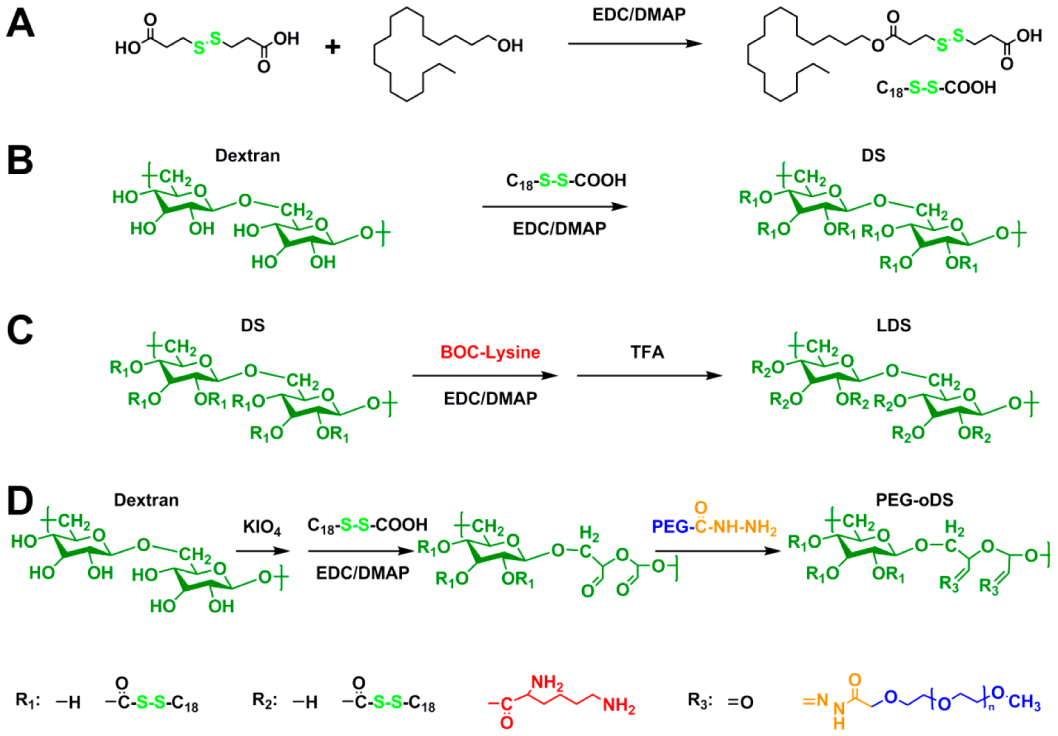


relatively low (approximately 2−20 μM). The disulfide bonds are prone to rapid cleavage under a reduction environment through thiol−disulfide exchange reactions.[16] Various reduction-sensitive nanocarriers based on disulfide bonds have been designed to realize triggered drug release in the tumor cells.[16,17]

Here, we report a kind of pH- and reduction-dual-responsive PEG coated polymeric lipid vesicles (PPLVs) that can achieve both enhanced tumor cellular internalization and triggered drug release. The PPLVs were based on amphiphilic modified dextran; PEG chains with pH-sensitive hydrazone bonds, stearyl alcohol (SA) chains with reduction-sensitive disulfide bonds, and positively charged lysine chains were connected to the dextran main chain. The antitumor drug, doxorubicin (DOX), was loaded in the cores of the PPLVs. As shown in Scheme 1, the nanosized PPLVs were modified with PEG on the surface, so they were neutral and had high colloidal stability in blood circulation. Once the DOX-loaded PPLVs reach tumor sites, they will lose their PEG coating by hydrolysis of hydrazone bonds under acidic tumor environments. Then the exposed positive charge could realize enhanced tumor cellular internalization. After the PPLVs are internalized by tumor cells, the PPLVs would disintegrate and release encapsulated DOX rapidly due to the cleavage of disulfide bonds in the presence of 2−10 mM GSH.

Herein we report our present study on the preparation and characterization of the PPLVs. The particle size, morphology, and *in vitro* drug release, as well as cellular uptake behaviors of the DOX-loaded PPLVs were investigated.

## 2. EXPERIMENTAL SECTION

**2.1. Materials.** Dextran ($M_w$ = 10000, Nanjing Duly Biotech Co., Ltd.), stearyl alcohol (SA, Sigma-Aldrich), poly(ethylene glycol) monomethyl ether (PEG, $M_n$ = 2000, Sigma-Aldrich), 3,3′-dithiodipropionic acid (Sigma-Aldrich), glutathione (GSH, Sigma-Aldrich), fluorescein isothiocyanate (FITC, Sigma-Aldrich), 4-(dimethylamino)pyridine (DMAP, Sigma-Aldrich), BOC−lysine (GL


dx.doi.org/10.1021/am502579e | ACS Appl. Mater. Interfaces 2014, 6, 10706−10713

Biochem Ltd.), *N*-(3-(dimethylamino)propyl)-*N*-ethylcarbodiimide hydrochloride (EDC·HCl, GL Biochem Ltd.), and doxorubicin hydrochloride (DOX, Beijing Zhongshuo Pharmaceutical Technology Development Co., Ltd.) were used as received.

**2.2. Synthesis of Dextran-S-S-SA (DS).** The $C_{18}$-*S*-*S*-COOH was first synthesized as shown in Scheme 2A. Briefly, 3,3′-dithiodipropionic acid (10 mmol) and EDC·HCl (11 mmol) were dissolved in 60 mL of *N*,*N*-dimethylformamide (DMF) and stirred for 30 min. SA (10 mmol) and DMAP (1 mmol) were dissolved in 72 mL of DMF/dichloromethane mixture (v/v = 5/1). Then the two solutions were mixed and stirred for 6 h at room temperature. After completion of the reaction, the solution was concentrated under reduced pressure and the obtained solution dialyzed (MWCO: 3500 Da) against pure water for 72 h and then lyophilized. DS was synthesized as shown in Scheme 2B. $C_{18}$-*S*-*S*-COOH (1200 mg), EDC·HCl (600 mg), and DMAP (100 mg) were dissolved in 48 mL of DMF/dichloromethane mixture (v/v = 5/1). Dextran (1000 mg) was dissolved in 20 mL of DMSO, and then the two solutions were mixed. The reaction mixture was stirred overnight at room temperature and then dialyzed (MWCO: 3500 Da) against ethanol for 48 h and then pure water for 72 h. Finally, the solution was lyophilized.

**2.3. Synthesis of Lysine-DS (LDS), PEG Conjugated Oxidized Dextran-S-S-SA (PEG-oDS), and FITC-DS.** The course of LDS preparation is shown in Scheme 2C. BOC-lysine (300 mg), EDC·HCl (200 mg), and DMAP (10 mg) were dissolved in 10 mL of DMSO and stirred for 30 min. DS (100 mg) was dissolved in 10 mL of DMSO and then added to the BOC-lysine solution. The solution was allowed to react for 12 h at room temperature. Then, the solution was dialyzed against pure water for 24 h to remove low molecular weight impurities. The dialyzed solution was lyophilized. Finally, the butyloxycarbonyl groups (BOC) on the lysine were removed by trifluoroacetic acid (TFA).

The course of PEG-oDS preparation is shown in Scheme 2D. Dextran was first oxidized by periodate oxidation and then reacted with $C_{18}$-*S*-*S*-COOH to obtain oDS. Then, oDS (100 mg) was dissolved in 20 mL of DMSO, and PEG-$CH_2CONHNH_2$ (200 mg; synthesized according to a published procedure[18]) was dissolved in another 15 mL of DMSO. Then, the two solutions were mixed, and the mixture was stirred under the protection of argon at 50 °C for 24 h, followed by dialyzing (MWCO: 3500 Da) against pure water for 24 h. The resulting solution was finally lyophilized.

FITC-DS was synthesized according to a published procedure.[19] DS (100 mg) was dissolved in 10 mL of DMSO, and then 20 mg of FITC was added. The mixture was stirred at 90 °C for 2 h in darkness. Then, the solution was dialyzed against pure water for 72 h and subsequently lyophilized.

**2.4. Characterization.** $^1$H NMR spectra were recorded on a JEOLGX 400 D spectrometer (400 MHz) with deuterated dimethyl sulfoxide as the solvent and tetramethyl silane as an internal standard at room temperature. To characterize the cleavage of hydrazone bonds and disulfide bonds under certain conditions, GSH was used to simulate the reduction (10 mM GSH) environment, and HCl was used to simulate the acidic (pH 5) environment. After 12 h of incubation, the degradation products were purified by dialysis against DMSO and pure water, and then lyophilized for $^1$H NMR analysis. The critical aggregation concentration (CAC) of DS in water was determined by a fluorescence probe technique (see Supporting Information).

**2.5. Preparation of PPLVs.** The PPLVs were prepared as follows: LDS (8 mg) and PEG-oDS (8 mg) were dissolved in 4 mL of dichloromethane. DOX (2 mg) was dissolved in 0.5 mL of pure water, and then the two solutions were mixed under sonication at 150 W output. After 30 s, the emulsion was added into 8 mL of pure water and sonicated for another 150 s. The organic solvent was then removed by rotary evaporation to form the PPLVs suspension. To prepare FITC-labeled PPLVs, FITC-DS (2 mg) was added into dichloromethane.

**2.6. Physicochemical Characterizations of the DOX-Loaded PPLVs.** The effective particle diameter and zeta potential of the DOX-loaded PPLVs were determined by dynamic light-scattering (DLS) at room temperature. Each experiment was repeated three times. The morphologies of the DOX-loaded PPLVs were observed by transmission electron microscopy (TEM). Suspensions of the DOX-loaded PPLVs were dropped on a carbon coated copper grid by negatively staining with 2% (w/v) phosphotungstic acid.

**2.7. Colloidal Stability Studies.** The colloidal stability of the PPLVs was investigated in DMEM with 10% fetal bovine serum (FBS) at the incubation temperature (37 °C). Effective particle diameters of the samples were monitored by DLS after 0, 30, 60, 90, and 120 min of incubation.

**2.8. Triggered Release of DOX *in Vitro*.** The *in vitro* triggered release profiles of the DOX-loaded PPLVs under different conditions were evaluated by a dialysis technique. Phosphate buffered solution (PBS) at pH 7.4 or acetate buffered solution (ABS) at pH 5.0 with or without 10 mM GSH was used as the environmental medium. In brief, 2 mL of the dispersed DOX-loaded PPLVs was added to dialysis bags (MWCO: 35000 Da) and placed in 10 mL of environmental media at 37 °C under constant shaking. At appropriate intervals, 5 mL of the environmental medium was taken out and replaced with the same amount of fresh medium. The amount of released DOX was measured using a UV spectrophotometer at a wavelength of 480 nm. Then, the accumulative ratios of the released DOX were calculated as a function of time.

**2.9. Cellular Uptake of FITC-Labeled PPLVs.** HeLa cells were seeded into 24-well plates ($3 \times 10^4$ cells/well) in 500 $\mu$L of complete Dulbecco's modified Eagle's medium (DMEM) with 10% FBS, followed by incubation at 37 °C for 24 h under 5% $CO_2$ atmosphere. Then, pretreated (at pH 5.0 or 7.4 for 3 h) FITC-labeled PPLVs were added. After incubation for 1 h, the culture media were removed, and the cells were washed twice by cold PBS. Thereafter, the cells were fixed with 4% (w/v) paraformaldehyde aqueous solution for 10 min and then stained with 4′,6-diamidino-2-phenylindole (DAPI, blue) for 15 min at room temperature. Then, the images of cells were observed using an inverted Olympus fluorescence microscope (IX-70), and the cellular uptake efficiency was analyzed by flow cytometry (FCM) for $1 \times 10^4$ cells.

**2.10. Cytotoxicity Assay.** The cytotoxicities of samples against HeLa cells were tested *in vitro* using an MTT-based assay. The cells were seeded into 96-well plates (4000 cells/well) in 100 $\mu$L of DMEM with 10% FBS, followed by incubation at 37 °C for 24 h under 5% $CO_2$ atmosphere. Then, 100 $\mu$L of medium containing the desired amount of samples was added. The cells were incubated for another 24 h at 37 °C. Then, 20 $\mu$L of MTT solution (5 mg/mL) was added to each well and incubation continued for another 4 h. The culture medium was removed, and 200 $\mu$L of DMSO was added into each well to dissolve the formazan. The absorbance of each well was measured at a test wavelength of 570 nm in a microplate reader (Model 680, Biorad). Survival percentage was then calculated as compared to that of untreated cells (100% survival).

## 3. RESULTS AND DISCUSSION

**3.1. Synthesis and Characterization of DS, LDS, and PEG-oDS.** The chemical structures of the prepared polymers were confirmed by $^1$H NMR. As shown in Figure S1B (Supporting Information), the peaks at $\delta$ (ppm) = 1.22 and 0.84, which were attributed to SA, were observed in the $^1$H NMR spectrum of DS. This result indicated that the DS was synthesized successfully. The peaks at $\delta$ (ppm) = 1.25−1.48 (attributed to lysine) and 3.49 (attributed to PEG) were also observed in $^1$H NMR spectra of LDS and PEG-oDS (Figure S1C and D, Supporting Information), respectively. All of these indicated that the polymers were synthesized successfully. The cleavage of hydrazone bonds and disulfide bonds in the specific environments was also measured by $^1$H NMR. As shown in Figure S2A (Supporting Information), after treatment with 10 mM GSH solution, the content of SA chains on the degradation products was decreased compared with that of DS, which indicated the cleavage of disulfide bonds. Similarly,

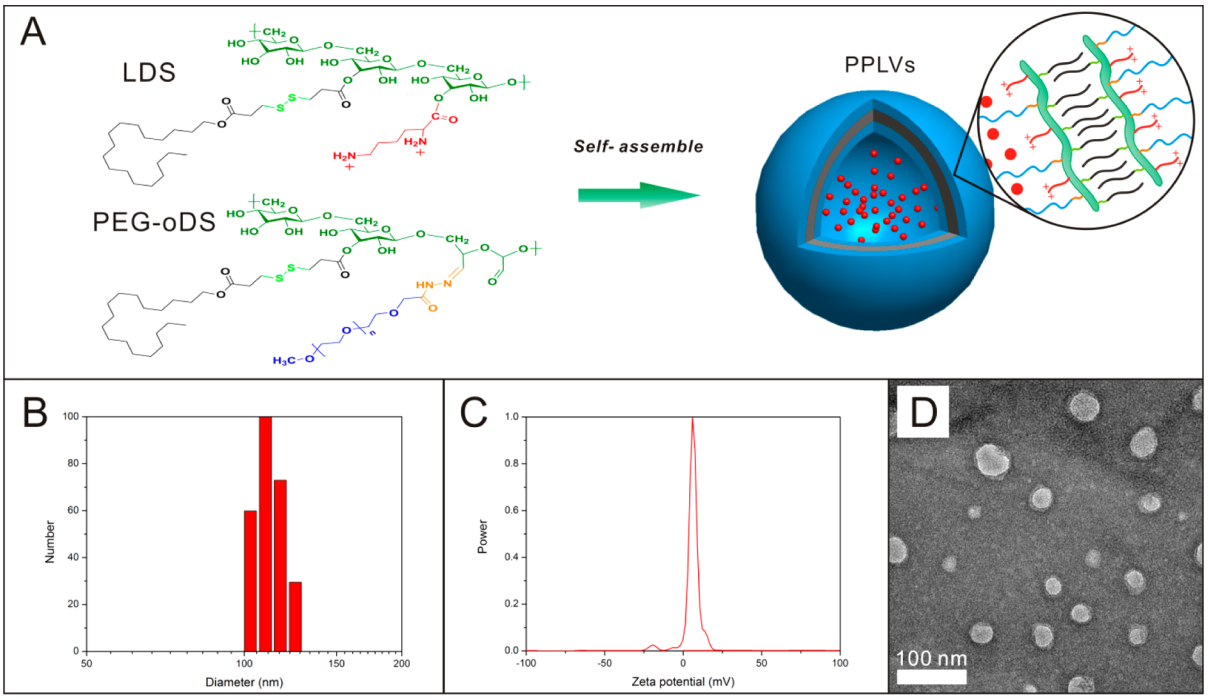


**Figure 1.** Preparation process (A), effective particle diameter (B), zeta potential (C), and TEM image (D) of the DOX-loaded PPLVs.

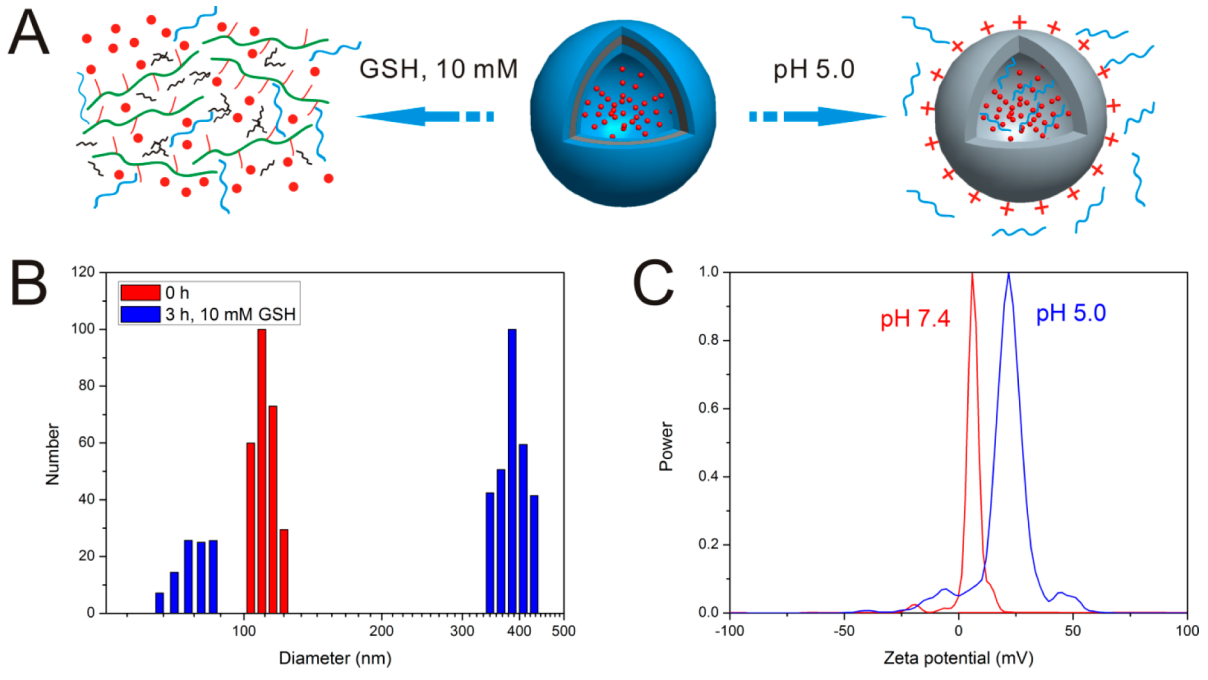


**Figure 2.** Schematic illustration of GSH-mediated disassembly and pH-activated surface charge switch of the DOX-loaded PPLVs (A); reduction-induced size change (B) and pH-induced surface charge switch (C) of the PPLVs.

the content of PEG chains was decreased after PEG-oDS was treated with HCl solution (Figure S2B, Supporting Information). These results suggested that the hydrazone bonds and disulfide bonds can be broken in the specific environments.

The CAC is a very important characteristic for amphiphilic polymers, indicating the polymer aggregate formation ability. Here, the CAC of DS was tested by a steady-state fluorescent probe study. The fluorescence emission spectrum of pyrene incorporated into DS in water was measured (Figure S3A, Supporting Information). As the concentration of DS increased, an abrupt increase in fluorescence intensity can be detected, which indicated the formation of aggregates and the transfer of pyrene into the hydrophobic core of the aggregates. The value of the $I_1/I_3$ ratio increased significantly with the transfer of pyrene molecules from a polar to a more hydrophobic microdomain. The CAC value of DS was determined from the intersection point of two straight lines (Figure S3B, Supporting Information) as about 38.19 mg/L, which indicated that the synthesized DS could easily self-assemble to form vesicles in aqueous medium.


dx.doi.org/10.1021/am502579e | ACS Appl. Mater. Interfaces 2014, 6, 10706−10713

**3.2. Formation and Characterization of the DOX-Loaded PPLVs.** The amphiphilic polymer could self-assemble in water under sonication to form vesicles. A schematic illustration for the preparation of DOX-loaded PPLVs is presented in Figure 1A. The effective particle diameter and zeta potential of the DOX-loaded PPLVs were characterized by DLS. Figure 1B and C summarized the effective particle diameter and zeta potential of the DOX-loaded PPLVs. The DOX-loaded PPLVs showed an effective particle diameter of 109.7 ± 8.6 nm and a zeta potential of 5.95 ± 2.69 mV. The morphology of the DOX-loaded PPLVs was investigated by TEM. As shown in Figure 1D, the DOX-loaded PPLVs were well dispersed as individual particles with a well-defined spherical structure and homogeneously distributed around 40 nm in diameter.

Figure 2A was a schematic illustration of GSH-mediated disassembly and pH-activated surface charge switch of the DOX-loaded PPLVs. To characterize the effective particle diameter and zeta potential changes of the DOX-loaded PPLVs in response to different conditions, the samples were treated with different solutions (pH 5.0 or 10 mM GSH) for 3 h before measurements. As shown in Figure 2B, effective particle diameter of the DOX-loaded PPLVs increased from 109.7 nm to about 380 nm after treatment with 10 mM GSH solution for 3 h. This reduction-induced fast aggregation behavior is due to the aggregation of hydrophobic molecules as a result of disulfide bonds cleavage. The PPLVs showed a zeta potential of 5.95 ± 2.69 mV in pH 7.4 solution. However, after treatment with pH 5.0 buffer solution for 3 h, the DOX-loaded PPLVs showed a zeta potential of 21.81 ± 5.94 mV (Figure 2C). This surface charge switch is mainly due to the shedding of the PEG coating as a result of hydrazone bond cleavage in acidic conditions.

**3.3. Colloidal Stability Studies.** The colloidal stability of the PPLVs was also examined by DLS. As a control, lysine-conjugated PLVs (LPLVs) were prepared by the same method as PPLVs preparation, but PEG-oDS was replaced with DS. The results of the effective particle diameters analysis are represented in Figure 3. The effective particle diameter of the PPLVs did not show any marked differences compared to the initial values after 120 min. However, the effective particle diameter of positively charged LPLVs started to increase in the first 30 min and reached a value of 247.8 nm after 120 min, which was 242.5% higher than their initial value. These results suggest that the PPLVs have low nonspecific adsorption rate and sufficient colloidal stability in circulation.

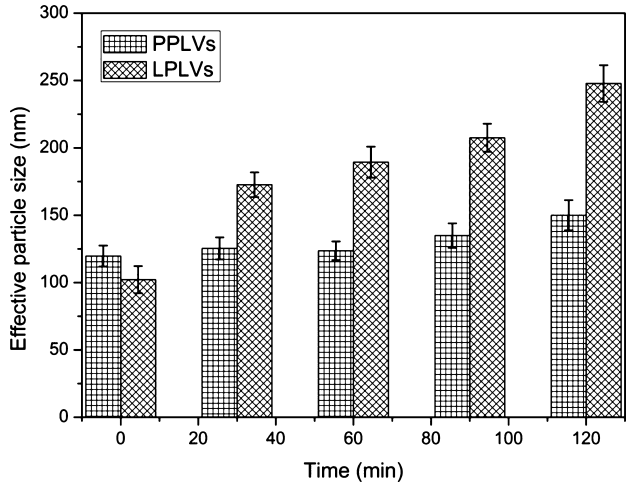


**Figure 3.** Colloidal stability in water of freshly prepared PPLVs and LPLVs versus DMEM + 10% FBS.

**3.4. Triggered Release of DOX *in Vitro*.** As chemotherapy drugs may cause severe adverse effects on healthy tissues, nanocarriers are expected to be stable before localizing in the tumor site, while releasing the encapsulated drugs rapidly after entering the tumor cells. To assess the triggered release behavior of the PPLVs, herein, the *in vitro* DOX release of the PPLVs was investigated using a dialysis bag (MWCO: 35000 Da) at 37 °C under four conditions: (i) pH 7.4, (ii) pH 5.0, (iii) pH 7.4 and 10 mM GSH, and (iv) pH 5.0 and 10 mM GSH. As shown in Figure 4A, only 24.0% DOX was released

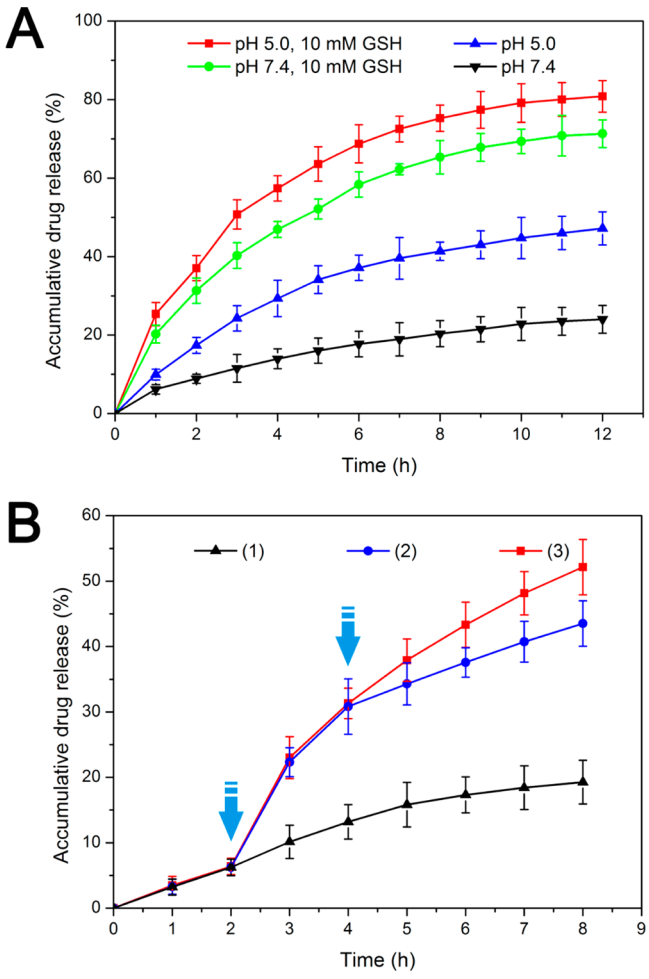


**Figure 4.** *In vitro* drug release profiles. (A) DOX-loaded PPLVs in various release media; (B) DOX-loaded PPLVs in three conditions: (1) pH 7.4, (2) pH 7.4 changed to pH 5.0 at 2 h, (3) pH 7.4 changed to pH 5.0 at 2 h and then GSH added to a concentration of 10 mM at 4 h.

from the DOX-loaded PPLVs in 12 h at the condition of pH 7.4. This result showed that the PPLVs have ideal stability under physiological pH conditions. The release of DOX was significantly accelerated at the condition of pH 5.0. In 12 h, 47.2% of DOX was released, likely due to pH-induced hydrolysis of hydrazone bonds. DOX was also released rapidly in response to a reduction environment containing 10 mM GSH, in which 71.3% and 80.8% of DOX was released in 12 h

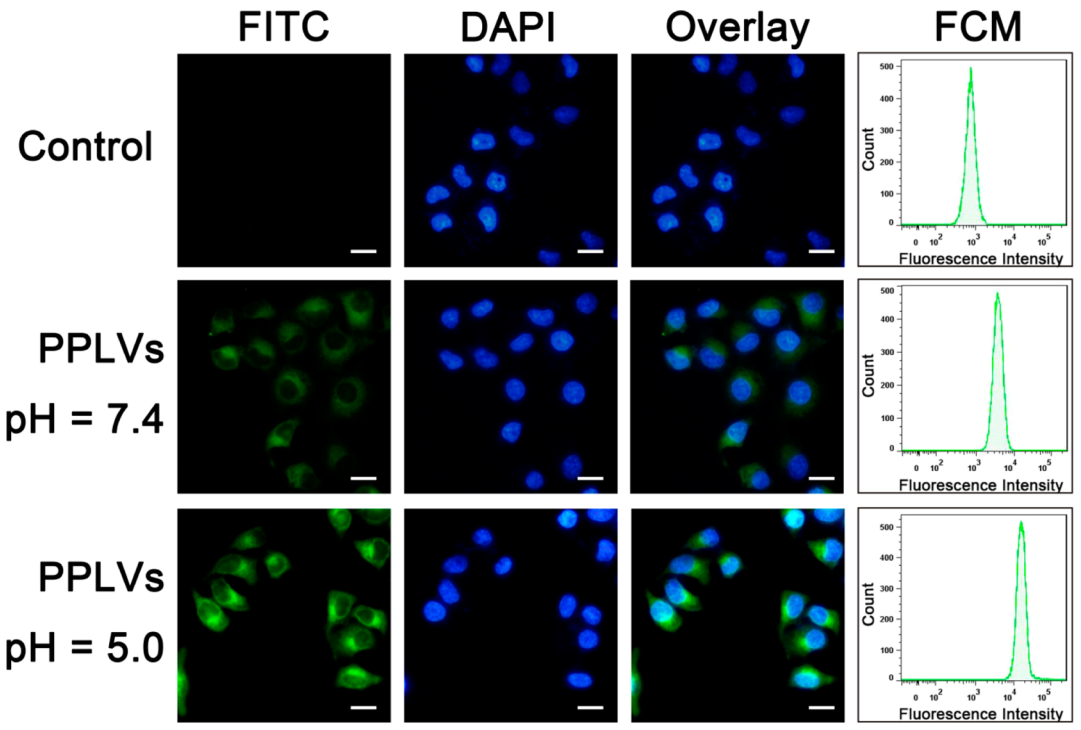


**Figure 5.** Fluorescence images and flow cytometry analyses of HeLa cells incubated with FITC-labeled PPLVs for 1 h. Scale bar: 10 $\mu$m.

at pH 7.4 and 5.0, respectively. In order to simulate the whole drug release behavior in the delivery process, drug release studies were performed as follows: at pH 7.4 (mimicking the environment of circulation) for 2 h and at pH 5.0 (mimicking the acidic environment of tumor sites) for another 2 h, and then at the pH 5.0 and 10 mM GSH condition (mimicking the acidic and reduction environments of tumor cells) for 4 h. As shown in Figure 4B, when the release media was changed at 2 and 4 h, the drug release speed was faster than that of control groups. All of these results suggest that the PPLVs can achieve triggered drug release in response to pH and reduction stimulation.

**3.5. Cellular Uptake of FITC-Labeled PPLVs *in Vitro*.** FITC was conjugated to the samples to observe the cellular uptake of PPLVs. The cellular uptake of samples was measured using fluorescence microscopy and flow cytometry. Untreated cells were used as a control.

As shown in the fluorescence images of HeLa cells (Figure 5), the fluorescence intensity of cells that were incubated with PBS (pH 7.4) pretreated PPLVs was relatively low. This result indicated that these PPLVs were difficult to take up by tumor cells, mainly because of the protection of the PEG coating that prevents them from contacting with cells. In contrast, the PPLVs with ABS (pH 5.0) pretreatment showed markedly higher fluorescence intensity within cells than the PPLVs with PBS pretreatment. This could possibly be due to the cleavage of hydrazone bonds caused by acid treatment because of which PPLVs lost their PEG coating. Then the exposed positive charge can be anchored to the cell surface through electrostatic binding.

The cellular uptake of FITC-labeled PPLVs was further studied by FCM. Figure 5 shows the mean FITC fluorescence intensity in HeLa cells after incubation with samples for 1 h. The cells incubated with the pH 5.0 pretreated PPLVs showed significantly increased fluorescence intensity when compared to that of those incubated with pH 7.4 pretreated PPLVs. The outcome was consistent with the fluorescence microscopy results.

**3.6. Cytotoxicity Assay.** To assess the cellular cytotoxicity of the DS, LDS, and PEG-oDS, HeLa cells were used. Following 24 h exposure to the samples, cell viabilities were assessed by the MTT assay. As shown in Figure 6, both DS and

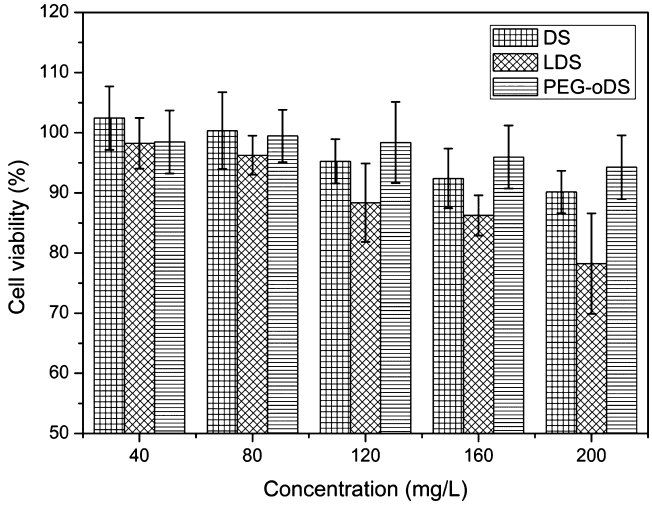


**Figure 6.** Cytotoxicity of DS, LDS, and PEG-oDS against HeLa cells following 24 h of incubation.

PEG-oDS were nontoxic to HeLa cells with cell viabilities more than 90% up to a tested concentration of 200 mg/L. However, with an increase in the concentration, the toxicity of the LDS increased. When the concentration of the LDS increased to 200 mg/L, the survival percentage of cells was only 78.2%. The cytotoxicity may be caused by the particularly high positive charge of LDS.

Antitumor activities of free DOX and DOX-loaded PPLVs with different solution treatments (pH 7.4 or 5.0) against HeLa cells following 24 h incubation were investigated. As shown in Figure 7, both free DOX and DOX-loaded PPLVs showed

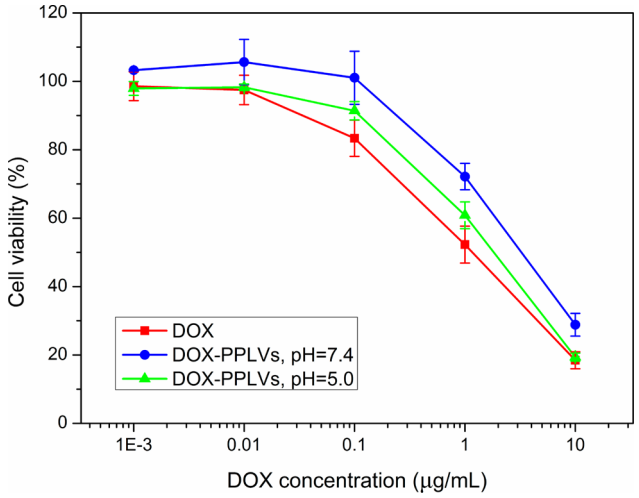


**Figure 7.** Antitumor activities of free DOX and the DOX-loaded PPLVs with different solutions treated (pH 7.4 or 5.0) against HeLa cells following 24 h of incubation as a function of DOX dosages.

DOX dose-dependent antitumor activities to HeLa cells. The DOX-loaded PPLVs exhibited lower antitumor activity than the free drug at the same dose of DOX, which may be due to the fact that water-soluble small molecule drugs can rapidly enter cells by passive diffusion. It should be noted that the $IC_{50}$ value of DOX-loaded PPLVs with pH 5.0 solution treatment (1.81 $\mu$g DOX/mL) was lower than that of DOX-loaded PPLVs with pH 7.4 solution treatment (3.19 $\mu$g DOX/mL). This high antitumor activity of DOX-loaded PPLVs with pH 5.0 solution treatment may be attributed to the enhanced cellular uptake efficiency as mentioned above. When the DOX-loaded PPLVs were treated with pH 5.0 solution, the pH-sensitive hydrazone bonds got hydrolyzed, and the protecting PEG coating was removed. The exposed positive lysine chains could realize enhanced tumor cellular internalization of the DOX-loaded PPLVs. After the internalization, DOX was released quickly due to the cleavage of disulfide bonds triggered by high GSH concentration in tumor cells.

## 4. CONCLUSIONS

In summary, a smart pH- and reduction-dual-responsive drug delivery system based on PPLVs was successfully fabricated. It has been demonstrated that the nanosized vesicles will lose their PEG coating as well as expose the positive charge under an acidic environment, thus efficiently entering tumor cells through electrostatic interactions. Furthermore, their structure will be broken in response to intracellular GSH levels, resulting in a triggered drug release in tumor cells. Therefore, PPLVs are promising carriers for smart antitumor drug delivery applications.

## ■ ASSOCIATED CONTENT

### Supporting Information

Further details of $^1$H NMR and CAC characterization of polymers. This material is available free of charge via the Internet at http://pubs.acs.org.

## ■ AUTHOR INFORMATION

### Corresponding Authors

*(H.W.) Tel: +86 022 87898212. E-mail: wanghj@tju.edu.cn.
*(J.C.) Tel: +86 022 87898212. E-mail: jinchang@tju.edu.cn.

### Notes

The authors declare no competing financial interest.

## ■ ACKNOWLEDGMENTS

The authors gratefully acknowledge National Natural Science Foundation of China (51373117, 51303126), Key Project of Tianjin Natural Science Foundation (13JCZDJC33200), National High Technology Program of China (2012AA022603), and Doctoral Base Foundation of Educational Ministry of China (20120032110027) for financial support of this work.

## ■ REFERENCES

(1) Peer, D.; Karp, J. M.; Hong, S.; Farokhzad, O. C.; Margalit, R.; Langer, R. Nanocarriers as an Emerging Platform for Cancer Therapy. *Nat. Nanotechnol.* **2007**, *2*, 751−760.
(2) Cheng, Z.; Al Zaki, A.; Hui, J. Z.; Muzykantov, V. R.; Tsourkas, A. Multifunctional Nanoparticles: Cost versus Benefit of Adding Targeting and Imaging Capabilities. *Science* **2012**, *338*, 903−910.
(3) Petros, R. A.; DeSimone, J. M. Strategies in the Design of Nanoparticles for Therapeutic Applications. *Nat. Rev. Drug Discovery* **2010**, *9*, 615−627.
(4) Wu, X.; Wang, Z.; Zhu, D.; Zong, S.; Yang, L.; Zhong, Y.; Cui, Y. pH and Thermo Dual-Stimuli-Responsive Drug Carrier Based on Mesoporous Silica Nanoparticles Encapsulated in a Copolymer-Lipid Bilayer. *ACS Appl. Mater. Interfaces* **2013**, *5*, 10895−10903.
(5) Zhang, Z.; Chen, X.; Chen, L.; Yu, S.; Cao, Y.; He, C.; Chen, X. Intracellular pH-Sensitive PEG-Block-Acetalated-Dextrans as Efficient Drug Delivery Platforms. *ACS Appl. Mater. Interfaces* **2013**, *5*, 10760−10766.
(6) Ernsting, M. J.; Murakami, M.; Roy, A.; Li, S. D. Factors Controlling the Pharmacokinetics, Biodistribution and Intratumoral Penetration of Nanoparticles. *J. Controlled Release* **2013**, *172*, 782−794.
(7) Wang, J.; Byrne, J. D.; Napier, M. E.; DeSimone, J. M. More Effective Nanomedicines through Particle Design. *Small* **2011**, *7*, 1919−1931.
(8) Zhao, F.; Zhao, Y.; Liu, Y.; Chang, X.; Chen, C.; Zhao, Y. Cellular Uptake, Intracellular Trafficking, and Cytotoxicity of Nanomaterials. *Small* **2011**, *7*, 1322−1337.
(9) Wang, H.; Zhao, P.; Liang, X.; Gong, X.; Song, T.; Niu, R.; Chang, J. Folate-PEG Coated Cationic Modified Chitosan−Cholesterol Liposomes for Tumor-Targeted Drug Delivery. *Biomaterials* **2010**, *31*, 4129−4138.
(10) Xiao, Y.; Jaskula-Sztul, R.; Javadi, A.; Xu, W.; Eide, J.; Dammalapati, A.; Kunnimalaiyaan, M.; Chen, H.; Gong, S. Co-delivery of Doxorubicin and siRNA Using Octreotide-Conjugated Gold Nanorods for Targeted Neuroendocrine Cancer Therapy. *Nanoscale* **2012**, *4*, 7185−7193.
(11) Chen, H.; Li, B.; Qiu, J.; Li, J.; Jin, J.; Dai, S.; Ma, Y.; Gu, Y. Thermal Responsive Micelles for Dual Tumor-Targeting Imaging and Therapy. *Nanoscale* **2013**, *5*, 12409−12424.
(12) Gratton, S. E. A.; Ropp, P. A.; Pohlhaus, P. D.; Luft, J. C.; Madden, V. J.; Napier, M. E.; DeSimone, J. M. The Effect of Particle Design on Cellular Internalization Pathways. *Proc. Natl. Acad. Sci. U.S.A.* **2008**, *105*, 11613−11618.
(13) Yuan, Z.; Que, Z.; Cheng, S.; Zhuo, R.; Li, F. pH-Triggered Blooming of 'Nano-flowers' for Tumor Intracellular Drug Delivery. *Chem. Commun.* **2012**, *48*, 8129−8131.
(14) Cheng, R.; Meng, F.; Deng, C.; Klok, H. A.; Zhong, Z. Dual and Multi-Stimuli Responsive Polymeric Nanoparticles for Programmed Site-Specific Drug Delivery. *Biomaterials* **2013**, *34*, 3647−3657.
(15) Shen, J. M.; Yin, T.; Tian, X. Z.; Gao, F. Y.; Xu, S. Surface Charge-Switchable Polymeric Magnetic Nanoparticles for the

Controlled Release of Anticancer Drug. *ACS Appl. Mater. Interfaces* **2013**, *5*, 7014−7024.
(16) Meng, F.; Hennink, W. E.; Zhong, Z. Reduction-Sensitive Polymers and Bioconjugates for Biomedical Applications. *Biomaterials* **2009**, *30*, 2180−2198.
(17) Ren, T.; Wu, W.; Jia, M.; Dong, H.; Li, Y.; Ou, Z. Reduction-Cleavable Polymeric Vesicles with Efficient Glutathione-Mediated Drug Release Behavior for Reversing Drug Resistance. *ACS Appl. Mater. Interfaces* **2013**, *5*, 10721−10730.
(18) Qiu, F.; Tu, C.; Chen, Y.; Shi, Y.; Song, L.; Wang, R.; Zhu, X.; Zhu, B.; Yan, D.; Han, T. Control of the Optical Properties of a Star Copolymer with a Hyperbranched Conjugated Polymer Core and Poly (ethylene glycol) Arms by Self-Assembly. *Chem.—Eur. J.* **2010**, *16*, 12710−12717.
(19) Wu, D. Q.; Lu, B.; Chang, C.; Chen, C. S.; Wang, T.; Zhang, Y. Y.; Cheng, S. X.; Jiang, X. J.; Zhang, X. Z.; Zhuo, R. X. Galactosylated Fluorescent Labeled Micelles as a Liver Targeting Drug Carrier. *Biomaterials* **2009**, *30*, 1363−1371.